Demonstration of Channel Multiplexing Quantum Communication Exploiting Entangled Sideband Modes

Shaoping Shi,[1,*] Long Tian,[1,2,*] Yajun Wang,[1,2] Yaohui Zheng,[1,2,†] Changde Xie,[1,2] and Kunchi Peng[1,2]
[1]State Key Laboratory of Quantum Optics and Quantum Optics Devices, Institute of Opto-Electronics, Shanxi University, Taiyuan 030006, China
[2]Collaborative Innovation Center of Extreme Optics, Shanxi University, Taiyuan 030006, China

(Received 17 November 2019; revised 18 March 2020; accepted 22 July 2020; published 14 August 2020)

Channel multiplexing quantum communication based on exploiting continuous-variable entanglement of optical modes offers great potential to enhance channel capacity and save quantum resource. Here, we present a frequency-comb-type control scheme for simultaneously extracting a lot of entangled sideband modes with arbitrary frequency detuning from a squeezed state of light. We experimentally demonstrate fourfold channel multiplexing quantum dense coding communication by exploiting the extracted four pairs of entangled sideband modes. Due to high entanglement and wide frequency separation between each entangled pairs, these quantum channels have large channel capacity and the cross talking effect can be avoided. The achieved channel capacities have surpassed that of all classical and quantum communication under the same bandwidth published so far. The presented scheme can be extended to more channels if more entangled sideband modes are extracted.

DOI: 10.1103/PhysRevLett.125.070502

After the continual exploration of theoretical and experimental physics during the past few decades, quantum information science, such as quantum dense coding [1–3], quantum key distribution [3–7], and quantum teleportation [3,8–11], is developing towards practical applications [12–14]. Saving quantum resource and enhancing capacity of quantum channels to the largest extent are common pursuits [15–17]. The concept of frequency division multiplexing quantum communication has been proposed by accessing N pairs of Einstein-Podolsky-Rosen (EPR) entangled sideband modes, in which only a broadband squeezed field is used for a quantum resource to provide a large number of quantum channels with narrow bandwidth [18,19]. The channel multiplexing quantum communication must allow multiple users to access the independent information without the crosstalk from each other [20]. Fifteen pairs of quadripartite entangled states were created by a dual-polarization optical parametric oscillator (OPO) [21]. With an OPO driven by a femtosecond pulse train, the entanglement of all possible bipartitions among ten spectral regions was shown [22]. Sixty modes were sequentially entangled into a dual-rail cluster state following polarization-domain protocol [23]. In all aforementioned experiments, the entangled sideband modes at different frequencies were not spatially separated and were detected in turn with corresponding frequency local oscillator (LO). Later, a pair of entangled sidebands with the entanglement degree of 3.8 dB was spatially separated from one squeezed field through a ring filter cavity without active stabilization [18,24]. Applying a pair of EPR entanglement sideband modes, the broadband improvement of gravitational-wave detectors has been demonstrated, which indicates a feasible method for future precise measurement [25–27]. Very recently, the channel multiplexing quantum communication based on single-photon entanglement has had a great progressing [28]. However, the development of channel multiplexing quantum communication with continuous variable (CV) entanglement of sideband modes of a squeezed field is not as quick as that for single photon system.

Although it has been shown that a single broadband squeezed field produced from an OPO is able to provide a large number (N) of quantum channels by utilizing distributed EPR entanglement between sideband modes [18,22,29,30], the multiplexing quantum communication with quantum channels of $N > 1$ based on CV EPR entanglement have not been realized experimentally so far. That is because the stable control scheme of entangled sideband modes has not been presented, which is a necessarily resolved problem before the application. In Ref. [18], the frequency beam splitter was not actively controlled and the orthogonal quadrature phases were locked in virtue of coherent amplitudes of the carrier field. Using this scheme, it is impossible to simultaneously manage many frequency beam splitters for scaling the higher mode number N and to utilize these sideband modes with frequencies far away from the carrier frequency. It is urgent to find an extensible control scheme of entangled sideband modes for realizing channel multiplexing quantum communication with high capacity of each channel and low cross talk between two neighboring channels.

Here we present a frequency-comb-type control scheme for simultaneous generation of more pairs of

EPR entangled sideband modes with arbitrary frequency detuning with respect to the carrier field. In virtue of the control scheme, we experimentally demonstrate channel multiplexing CV quantum dense coding communication, in which four pairs of entangled sideband modes of a single squeezed field are spatially separated and then used for information transmission between two independent pairs of distant users. Fourfold entangled sideband modes, respectively, with high entanglement of 8.0, 7.9, 7.2, and 7.6 dB are spatially separated at the first four resonances of OPO. Since the four quantum channels are located at different resonances of the OPO with the large frequency intervals, the cross talking effect can be totally avoided. The achieved channel capacities surpass that of all other quantum communication with the same bandwidth, such as coherent state, squeezed state and Fock state [31] communication. According to the presented scheme, a CV multiplexing quantum communication involving more users can be realized by a single quantum resource of squeezed state.

The schematic diagram of the channel multiplexing quantum communication is shown in Fig. 1. Squeezed states have fewer fluctuations in one quadrature than vacuum noise at the expense of increased fluctuations in the other quadrature [32]. The squeezing of a broadband squeezed field derives from quantum correlations between each pair of symmetric sidebands around the half pump frequency ω_0 [22]. In other words, a squeezed field involves a lot of EPR entangled modes at these sidebands of $\omega_{\pm i}$ $(i = 1, 2, n)$ within the spectral acceptance of nonlinear crystal [23] and the frequency separation between two adjacent modes is a free spectral range of OPO cavity. Each pair of sideband modes can be used for an independent quantum channel for quantum communication, the spectrum bandwidth of which is determined by the linewidth of the OPO. The upper sidebands are distributed to the senders for performing signal encoding. After the demultiplexing operation with a cascade of bandpass filters, the transmitted signals of each sender are independently encoded on one of the separated upper sideband modes (ω_{+1}, ω_{+2}, ω_{+n}), respectively. These encoded signals may be submerged in huge thermal noise of a half of EPR mode [33], such that the unauthorized receiver without holding the other half of the EPR mode cannot retrieve the transmitted signal. The lower sidebands (ω_{-1}, ω_{-2}, ω_{-n}) are transmitted to distant receivers after demultiplexing. Then, each receiver demodulates the received signals using the other half of EPR modes held by them, independently. Due to the use of EPR entanglement, the signal-to-noise ratio (SNR) of signals decoded by each receiver can break through the corresponding shot noise limit (SNL) [34].

With the experimental setup shown in Fig. 2, we implement the four-channel multiplexing quantum communication applying four pairs of EPR sideband modes from a squeezed field. The squeezed state of light is generated by a below-threshold OPO operating at deamplification state, which has been analyzed in detail in our previous publications [35,36]. A cascade of seven triangular-shaped ring filter cavities is employed as the bandpass

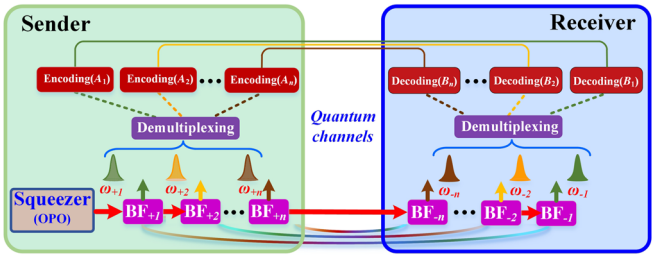

FIG. 1. Schematic diagram of the channel multiplexing quantum communication. Squeezed light source (squeezer) is an OPO pumped by a continuous-wave single-frequency laser, the output spectrum is then split by two sets of cascade bandpass filters (BF_{+i} and BF_{-i}, $i = 1, 2, n$). In Sender, different signals are individually encoded on different sidebands. At Receiver, modes (A_1, A_2, A_n) after demultiplexing, these transmitted signals are, respectively, decoded with the help of the other half of corresponding EPR entangled sideband modes by different users (B_1, B_2, B_n).

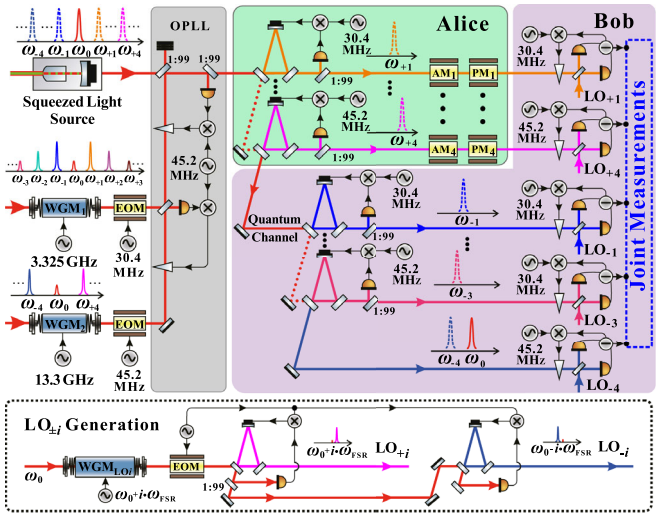

FIG. 2. Experimental setup of the channel multiplexing quantum communication. At sender station (Alice), four sets of the classical amplitude and phase signals are modulated on sideband modes ω_{+1}, ω_{+2}, ω_{+3}, and ω_{+4}, and then are independently sent to the receiver station (Bob). The four sideband modes ω_{-1}, ω_{-2}, ω_{-3}, and ω_{-4} are sent to the receiver station through one frequency multiplexing channel, where after demultiplexing they are respectively distributed to four users. Then, the four users decode the signals carried by sideband modes ω_{+1}, ω_{+2}, ω_{+3}, and ω_{+4} under the help of four sideband modes ω_{-1}, ω_{-2}, ω_{-3}, and ω_{-4}, respectively. The decoding was performed by four sets of balanced homodyne detectors; WGM, waveguide electro-optic modulator; EOM, electro-optic modulator; OPLL, optical phase locking loop; AM, amplitude modulator; PM, phase modulator; LO, local oscillator.

filters to separate these sideband modes. Seven filter cavities resonate with each sideband modes at one of frequencies $\omega_{+1}, ..., \omega_{+4}$ and ω_{-1}, ω_{-2}, ω_{-3}, respectively, thus a corresponding frequency component is transmitted from a filter cavity. In order to reduce the decoherence resulting from losses, we consider synthetically the influences of impedance matching, linewidth, and sideband suppression ratio of filter cavity on the EPR sideband entanglement in the design and building of filter cavity (for details, see the Supplemental Material [37]). Since there are no enough coherent amplitudes at these sideband modes of an optical squeezed state, the extraction of these signals, which are needed for actively these filter cavities and relative phases between local oscillators and signals in the downstream experiment [43,44], is impossible.

In order to solve the problem, we design a generation system of auxiliary control beams by employing two fiber-coupled waveguide electro-optic modulators (WGM_1 and WGM_2). WGM_1 with a modulation frequency (amplitude) of 3.325 GHz (26 dBm) simultaneously generates sideband modes $\omega_{\pm1}$, $\omega_{\pm2}$, and $\omega_{\pm3}$. WGM_2 with a modulation frequency (amplitude) of 13.3 GHz (22 dBm) produces the sideband modes $\omega_{\pm4}$. The two modulation frequencies equal to one and four times of the free spectral range of OPO, respectively. When we tune the modulation frequency starting from zero, the first-order sideband of WGM is shifted until the transmission peak overlaps with the carrier first. At that particular moment, the modulation frequency is recorded, which equals to the free spectral range of OPO. The carrier fields of WGM_1 and WGM_2 are phase locked by an optical phase locking loop. In this way, the obtained auxiliary control beam involves many optical modes with different frequencies ($\omega_{\pm1}$, $\omega_{\pm2}$, $\omega_{\pm n}$) just like an optical frequency comb. The comb teeth corresponding to the first four resonances of the OPO have a phase difference of 0 or π with the carrier. On the other hand, the phase difference between a sideband mode of the squeezed state generated by the OPO and seed beam injected into the OPO is also 0 or π. Therefore, when the phase of the carrier of the auxiliary control beam is locked in that of the transmitted seed beam, the relative phases between each sideband and its corresponding auxiliary control beam at the same frequency are naturally locked. The power of the seed beam transmitted from the OPO is about 45 μW, which is enough to be used for optical phase-locking loop (for details, see supplemental material [37]). Combining each vacuum sideband mode of a squeezed state and a corresponding auxiliary control beam at the same frequency and phase, vacuum sideband modes are converted to the bright optical modes by coherent amplitudes, which can be utilized to manage the downstream filter cavities and balanced homodyne detections (BHDs). Besides, the bright sideband modes can also be directly encoded by amplitude and phase modulators, to implement conveniently quantum communication [37].

For implementing BHDs on sideband modes of a squeezed state at $\omega_{\pm i}$ ($i = 1$–4), four pairs of LOs at $\omega_0 \pm \omega_{\mathrm{FSR}}$, $\omega_0 \pm 2\omega_{\mathrm{FSR}}$, $\omega_0 \pm 3\omega_{\mathrm{FSR}}$, and $\omega_0 \pm 4\omega_{\mathrm{FSR}}$ have to be prepared. These LOs with different frequencies are also generated by four waveguide electro-optical modulators (WGM_{LO1}, WGM_{LO2}, WGM_{LO3}, and WGM_{LO4}) driven by radio frequency sources at ω_{FSR}, $2\omega_{\mathrm{FSR}}$, $3\omega_{\mathrm{FSR}}$, and $4\omega_{\mathrm{FSR}}$, and subsequent optical mode cleaners, respectively, where ω_{FSR} is the free spectral range of the OPO. An optical mode cleaner consists of two plane mirrors and one curved mirror with the round-trip length of 232.0 mm, and the curved cavity mirror shows a transmissivity of 0.008% with the curvature radius of 1.0 m. The two plane cavity mirrors have a power transmissivity of 0.5% for s-polarized beam, corresponding to the finesse value of 620 and linewidth of 2 MHz. The optical mode cleaner has a power transmission of 81% for the resonant sideband and less than 0.001% for the carrier and non-resonant sidebands, thus the suppression factor of about 10^5 for the carrier and other sideband modes is obtained, which is enough to be used to measure the quadrature operators without any interference. Two optical mode cleaners after each WGM resonant successively with the sidebands $\omega_0 + \omega_{\mathrm{FSR}}$ and $\omega_0 - \omega_{\mathrm{FSR}}$, the transmitted sideband is solely picked out [37]. All of these locking loops are constructed by a Pound-Drever-Hall technique and error signals are extracted by resonant photodetectors with high Q value to reduce the loss of signal extraction as much as possible.

The correlation noises of amplitude sum and phase difference between the upper and lower sidebands measured by BHDs are shown in Fig. 3. The variances of amplitude sum and phase difference are unbiased and equal to 8.0, 7.9, 7.2, and 7.6 dB for $\omega_{\pm1}$, $\omega_{\pm2}$, $\omega_{\pm3}$, and $\omega_{\pm4}$, respectively, without the correct of the electronic noise, which are the first report of the simultaneous measurement of four EPR sideband entanglement pairs. The small reduction of quantum correlation from $\omega_{\pm1}$ to $\omega_{\pm4}$ is mainly caused by the loss of cascade filter cavities and additional loss of error signal extraction, but not limited by the spectral acceptance bandwidth of periodically poled $KTiOPO_4$, thus it can be further improved by decreasing the loss of filter cavities and improving the performance of control loop. The generated four pairs of EPR entangled sideband beams well satisfy the inseparable criteria [45] of $\mathrm{Var}(\hat{X}_A + \hat{X}_B) + \mathrm{Var}(\hat{Y}_A - \hat{Y}_B) < 2$. The measured correlation variances in the left of the inequality are 0.314 for $\omega_{\pm1}$, 0.324 for $\omega_{\pm2}$, 0.381 for $\omega_{\pm3}$, and 0.348 for $\omega_{\pm4}$, respectively. Such a high entanglement level for four pairs of sideband modes provides the fundamental physical condition to accomplish the channel multiplexing quantum communication with large channel capacity.

The frequencies of signals are 2 MHz at ω_{+1}, 1.5 MHz at ω_{+2}, 1.6 MHz at ω_{+3}, and 1.8 MHz ω_{+4}, respectively. The noise level of each half of the EPR beam is 16 dB above

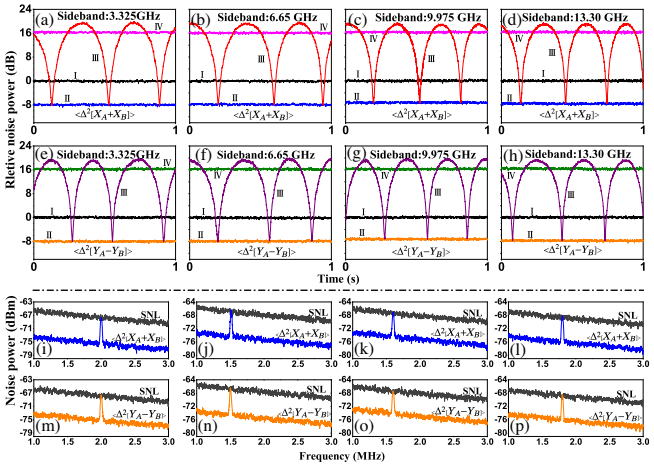

FIG. 3. Spectral densities of amplitude sum (a)–(d) and phase difference (e)–(h) at the first, second, third, and fourth resonances of the OPO. With the signal ports of the two BHDs blocked, the output of the power combiners corresponds to the SNL (trace I). When the relative phases between the LOs and two sidebands of squeezed states are 0 ($\pi/2$), the outputs of two corresponding BHDs are combined with the positive (subtractive) power combiners to obtain the noise powers of amplitude sum (phase difference) are show in trace II. One of the BHD's phases keeps constant while another BHD's phase is scanned linearly in time, the corresponding noise variance is shown in trace III. When one of the BHD signal port is blocked, the noise spectrum is higher than the SNL, which is insensitive to the relative phase (trace IV). Measured amplitude (i)–(l) and phase (m)–(p) signal at Bob, when the encoding signals at Alice are 2, 1.5, 1.6, and 1.8 MHz at the first four resonances of the OPO, indicating that four users have no experiencing interference.

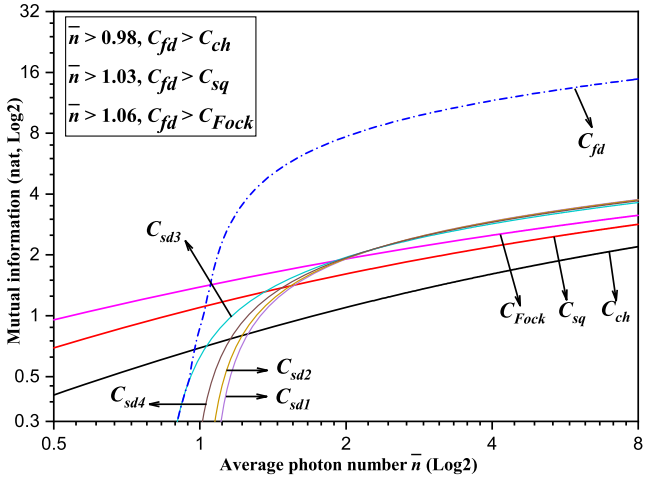

FIG. 4. Channel capacity by various channels, measured by mutual information as functions of the average photon number $\bar{n}$. Shown are coherent state channel C_{ch}, squeezed state channel with optimized noise variance C_{sq}, Holevo limit of a single-mode bosonic channel C_{Fock}, single dense coding channel inferred with measured entanglement degree C_{sd1} (C_{sd2}, C_{sd3}, C_{sd4}), and fourfold multiplexing channel C_{fd} with the sum of C_{sd1}, C_{sd2}, C_{sd3}, and C_{sd4}. The amount of information is presented in nat $= (1/\ln 2)$bit.

that of the corresponding SNL. It is obvious that the extraction of signals merged in the large noise background is quite difficult if without the help of the other half of the EPR beam. With the aid of the EPR beam, the signals are retrieved with the SNR of 7.8, 7.7, 7.1, and 7.5 dB beyond the SNL for both amplitude and phase quadratures at four logic channels, respectively, shown in Fig. 3. For the first time, our experiments have demonstrated fourfold channel multiplexing quantum communication in virtue of the frequency-comb-type control scheme.

Using the above measured SNRs, we evaluate the capacities of channel multiplexing quantum communication. Figure 4 shows the comparison of the channel capacity at various channels, which are calculated with the formulas in Refs. [31,46–48]. We can see that for each channel, the channel capacity of the quantum dense coding communication has exceeded that of other CV quantum communication protocols, such as coherent state C_{ch}, squeezed state with the optimal value C_{sq}, Fock state communication C_{Fock}, which is the Holevo limit of a single-mode bosonic channel, under the condition of $\bar{n} > 2.01$, 1.99, 1.90, 1.95 ($\bar{n}$ stands for the average photon number), respectively [31]. The channel multiplexing further increases the total capacity, thus this scheme opens a new road to boost up the channel capacity of a communication system. If we combine the advantage of the time domain multiplexing [48–50], according to the technology used in classical communication [51], the number of the channel multiplexing is expected to scale to a higher level.

In conclusion, we have reported a frequency-comb-type control scheme that allowed a simultaneous generation and application of more pairs of entangled sideband modes with arbitrary frequency detuning. A channel multiplexing quantum communication exploiting fourfold EPR entangled sideband modes from a single squeezed field has been demonstrated for the first time. It is worthy to note that the control scheme is able to be extended to the generation of more entangled sideband modes according to the requests of a practical quantum communication. The presented control scheme is an important step toward developing scalable channel multiplexing quantum communication. Based on the use of a squeezed state, the channel multiplexing quantum communication involving a large number of users with high capacity can be realized by increasing classical devices to extend the present system. If the presented control scheme combines with the filter cavity of waveguide [52], and integrated silicon-based material [53–55], the compact channel multiplexing quantum communication with large number of N will possibly be accomplished.

We acknowledge financial support from the National Natural Science Foundation of China (NSFC) (Grants No. 11654002, No. 61575114, No. 11804207, and No. 11874250); National Key R&D Program of China

(Grant No. 2016YFA0301401); Key R&D Program of Shanxi (Grant No. 201903D111001); Program for Sanjin Scholar of Shanxi Province; Program for Outstanding Innovative Teams of Higher Learning Institutions of Shanxi; Fund for Shanxi 1331 Project Key Subjects Construction.

*These authors contributed equally to this work.
†yhzheng@sxu.edu.cn.

[1] K. Mattle, H. Weinfurter, P. G. Kwiat, and A. Zeilinger, Dense Coding in Experimental Quantum Communication, Phys. Rev. Lett. **76**, 4656 (1996).
[2] S. L. Braunstein and H. J. Kimble, Dense coding for continuous variables, Phys. Rev. A **61**, 042302 (2000).
[3] S. L. Braunstein and P. V. Loock, Quantum information with continuous variables, Rev. Mod. Phys. **77**, 513 (2005).
[4] H.-K. Lo, M. Curty, and K. Tamaki, Secure quantum key distribution, Nat. Photonics **8**, 595 (2014).
[5] H.-K. Lo, M. Curty, and B. Qi, Measurement-Device-Independent Quantum Key Distribution, Phys. Rev. Lett. **108**, 130503 (2012).
[6] F. Grosshans, G. Van Assche, J. Wenger, R. Brouri, N. J. Cerf, and P. Grangier, Quantum key distribution using Gaussian-modulated coherent states, Nature (London) **421**, 238 (2003).
[7] N. Wang, S. N. Du, W. Y. Liu, X. Y. Wang, Y. M. Li, and K. C. Peng, Long-Distance Continuous-Variable Quantum Key Distribution with Entangled States, Phys. Rev. Applied **10**, 064028 (2018).
[8] A. Furusawa, J. L. Srensen, S. L. Braunstein, C. A. Fuchs, H. J. Kimble, and E. S. Polzik, Unconditional quantum teleportation, Science **282**, 706 (1998).
[9] S. L. Braunstein and H. J. Kimble, Teleportation of Continuous Quantum Variables, Phys. Rev. Lett. **80**, 869 (1998).
[10] D. Bouwmeester, J.-W. Pan, K. Mattle, M. Eibl, H. Weinfurter, and A. Zeilinger, Experimental quantum teleportation, Nature (London) **390**, 575 (1997).
[11] S. Pirandolar, J. Eisert, C. Weedbrook, A. Furusawa, and S. L. Braunstein, Advances in quantum teleportation, Nat. Photonics **9**, 641 (2015).
[12] B. Korzh, C. C. W. Lim, R. Houlmann, N. Gisin, M. J. Li, D. Nolan, B. Sanguinetti, R. Thew, and H. Zbinden, Provably secure and practical quantum key distribution over 307 km of optical fibre, Nat. Photonics **9**, 163 (2015).
[13] R. Ursin, F. Tiefenbacher, T. Schmitt-manderbach, H. Weier, T. Scheidl, M. Lindenthal, B. Blauensteiner, T. Jennewein, J. Perdigues, P. Trojek, B. Omer, M. Furst, M. Meyenburg, J. Rarity, Z. Sodnik, C. Barbieri, H. Weinfurter, and Z. Zeilinger, Entanglement-based quantum communication over 144 km, Nat. Phys. **3**, 481 (2007).
[14] S. K. Liao *et al.*, Satellite to ground quantum key distribution, Nature (London) **549**, 43 (2017).
[15] A. Grudka and A. Wjcik, Symmetric scheme for superdense coding between multiparties, Phys. Rev. A **66**, 014301 (2002).
[16] X. S. Liu, G. L. Long, D. M. Tong, and F. Li, General scheme for superdense coding between multiparties, Phys. Rev. A **65**, 022304 (2002).
[17] X. Y. Li, Q. Pan, J. T. Jing, J. Zhang, C. D. Xie, and K. C. Peng, Quantum Dense Coding Exploiting a Bright Einstein-Podolsky-Rosen Beam, Phys. Rev. Lett. **88**, 047904 (2002).
[18] B. Hage, A. Samblowski, and R. Schnabel, Towards Einstein-Podolsky-Rosen quantum channel multiplexing, Phys. Rev. A **81**, 062301 (2010).
[19] H. B. Song, H. Yonezawa, K. B. Kuntz, M. Heurs, and E. H. Huntington, Quantum teleportation in space and frequency using entangled pairs of photons from a frequency comb, Phys. Rev. A **90**, 042337 (2014).
[20] M. Heurs, J. G. Webb, A. E. Dunlop, C. C. Harb, T. C. Ralph, and E. H. Huntington, Multiplexed communication over a high-speed quantum channel, Phys. Rev. A **81**, 032325 (2010).
[21] M. Pysher, Y. Miwa, R. Shahrokhshahi, R. Bloomer, and O. Pfister, Parallel Generation of Quadripartite Cluster Entanglement in the Optical Frequency Comb, Phys. Rev. Lett. **107**, 030505 (2011).
[22] J. Roslund, R. Medeiros, S. F. Jiang, C. Fabre, and N. Treps, Wavelength-multiplexed quantum networks with ultrafast frequency combs, Nat. Photonics **8**, 109 (2014).
[23] M. Chen, N. C. Menicucci, and O. Pfister, Experimental Realization of Multipartite Entanglement of 60 Modes of a Quantum Optical Frequency Comb, Phys. Rev. Lett. **112**, 120505 (2014).
[24] C. Schori, J. L. Sorensen, and E. S. Polzik, Narrow-band frequency tunable light source of continuous quadrature entanglement, Phys. Rev. A **66**, 033802 (2002).
[25] Y. Ma, H. Miao, B. H. Pang, M. Evans, C. Zhao, J. Harms, R. Schnabel, and Y. Chen, Proposal for gravitational-wave detection beyond the standard quantum limit through EPR entanglement, Nat. Phys. **13**, 776 (2017).
[26] M. J. Yap, P. Altin, T. G. McRae, B. J. J. Slagmolen, R. L. Ward, and D. E. McClelland, Generation and control of frequency-dependent squeezing via Einstein-Podolsky-Rosen entanglement, Nat. Photonics **14**, 223 (2020).
[27] J. Sdbeck, S. Steinlechner, M. Korobko, and R. Schnabel, Demonstration of interferometer enhancement through Einstein-Podolsky-Rosen entanglement, Nat. Photonics **14**, 240 (2020).
[28] S. Wengerowsky, S. Koduru, F. Steinlechner, H. Hubel, and R. Ursin, An entanglement-based wavelength-multiplexed quantum communication network, Nature (London) **564**, 225 (2018).
[29] J. Zhang, Einstein-Podolsky-Rosen sideband entanglement in broadband squeezed light, Phys. Rev. A **67**, 054302 (2003).
[30] E. H. Huntington and T. C. Ralph, Separating the quantum sidebands of an optical field, J. Opt. B **4**, 123 (2002).
[31] J. Mizuno, K. Wakui, A. Furusawa, and M. Sasaki, Experimental demonstration of entanglement-assisted coding using a two-mode squeezed vacuum state, Phys. Rev. A **71**, 012304 (2005).
[32] G. Breitenbach, S. Schiller, and J. Mlynek, Measurement of the quantum states of squeezed light, Nature (London) **387**, 471 (1997).
[33] S. F. Pereira, Z. Y. Ou, and H. J. Kimble, Quantum communication with correlated nonclassical states, Phys. Rev. A **62**, 042311 (2000).
[34] Z. Y. Ou, S. F. Pereira, and H. J. Kimble, Realization of the Einstein-Podolsky-Rosen paradox for continuous variables

in nondegenerate parametric amplification, Appl. Phys. B **55**, 265 (1992).

[35] W. H. Yang, S. P. Shi, Y. J. Wang, W. G. Ma, Y. H. Zheng, and K. C. Peng, Detection of stably bright squeezed light with the quantum noise reduction of 12.6 dB by mutually compensating the phase fluctuations, Opt. Lett. **42**, 4553 (2017).

[36] S. P. Shi, Y. J. Wang, W, H. Yang, Y. H. Zheng, and K. C. Peng, Detection and perfect fitting of 13.2 dB squeezed vacuum states by considering green-light-induced-infrared absorption, Opt. Lett. **43**, 5411 (2018).

[37] See the Supplemental Material at http://link.aps.org/supplemental/10.1103/PhysRevLett.125.070502, for control scheme for downstream ring filter cavities and detection phases, entanglement bandwidth of the optical frequency comb in a single broadband squeezed field and ring filter cavity for the separation of sideband fields, which includes Refs. [18,35,38–42].

[38] C. Y. Chen, Z. X. Li, X. L. Jin, and Y. H. Zheng, Resonant photodetector for cavity- and phase-locking of squeezed state generation, Rev. Sci. Instrum. **87**, 103114 (2016).

[39] J. R. Wang, W. H. Zhang, L. Tian, Y. J. Wang, R. C. Yang, J. Su, and Y. H. Zheng, Balanced homodyne detector with independent phase control and noise detection branches, IEEE Access **7**, 57054 (2019).

[40] L. E. Myers, R. C. Eckardt, M. M. Fejer, R. L. Byer, W. R. Bosenberg, and J. W. Pierce, Quasi-phase-matched optical parametric oscillators in bulk periodically poled $LiNbO_3$, J. Opt. Soc. Am. B **12**, 2102 (1995).

[41] R. W. Boyd, *Nonlinear Optics*, 3rd revised ed. (Academic Press, New York, 2008), ISBN 0123694701.

[42] P. Barriga, C. Zhao, and D. G. Blair, Optical design of a high power mode-cleaner for AIGO, Gen. Relativ. Gravit. **37**, 1609 (2005).

[43] H. Vahlbruch, S. Chelkowski, B. Hage, A. Franzen, K. Danzmann, and R. Schnabel, Coherent Control of Vacuum Squeezing in the Gravitational-Wave Detection Band, Phys. Rev. Lett. **97**, 011101 (2006).

[44] H. Vahlbruch, A. Khalaidovski, N. Lastzka, C. Graf, K. Danzmann, and R. Schnabel, The GEO600 squeezed light source, Classical Quantum Gravity **27**, 084027 (2010).

[45] L. M. Duan, G. Giedke, J. I. Cirac, and P. Zoller, Inseparability Criterion for Continuous Variable Systems, Phys. Rev. Lett. **84**, 2722 (2000).

[46] T. C. Ralph and E. H. Huntington, Unconditional continuous-variable dense coding, Phys. Rev. A **66**, 042321 (2002).

[47] J. T. Jing, J. Zhang, Y. Yan, F. G. Zhao, C. D. Xie, and K. C. Peng, Experimental Demonstration of Tripartite Entanglement and Controlled Dense Coding for Continuous Variables, Phys. Rev. Lett. **90**, 167903 (2003).

[48] S. Yokoyama, R. Ukai, S. C. Armstrong, C. Sornphiphatphong, T. Kaji, S. Suzuki, J. I. Yoshikawa, N. C. Menicucci, and A. Furusawa, Ultra-large-scale continuous-variable cluster states multiplexed in the time domain, Nat. Photonics **7**, 982 (2013).

[49] M. V. Larsen, X. S. Guo, C. R. Breum, J. S. Neergaard-Nielsen, and U. L. Andersen, Deterministic generation of a two-dimensional cluster state, Science **366**, 369 (2019).

[50] W. Asavanant, Y. Shiozawa, S. Yokoyama, B. Charoensombutamon, H. Emura, R. N. Alexander, S. Takeda, J. Yoshikawa1, N. C. Menicucci, H. Yonezawa, and A. Furusawa, Generation of time-domain-multiplexed two-dimensional cluster state, Science **366**, 373 (2019).

[51] G. Fettweis, M. Krondorf, and S. Bittner, GFDM—Generalized frequency division multiplexing, in *Proceedings of the VTC Spring 2009 - IEEE 69th Vehicular Technology Conference, Barcelona* (IEEE, 2009), pp. 1–4, https://dx.doi.org/10.1109/VETECS.2009.5073571.

[52] M. Stefszky, R. Ricken, C. Eigner, V. Quiring, H. Herrmann, and C. Silberhorn, Waveguide Cavity Resonator as a Source of Optical Squeezing, Phys. Rev. Applied **7**, 044026 (2017).

[53] A. Dutt, S. Miller, K. Luke, J. Cardenas, A. L. Gaeta, P. Nussenzveig, and M. Lipson, Tunable squeezing using coupled ring resonators on a silicon nitride chip, Opt. Lett. **41**, 223 (2016).

[54] J. S. Levy, A. Gondarenko, M. A. Foster, A. C. Turner-Foster, A. L. Gaeta, and M. Lipson, CMOS-compatible multiple-wavelength oscillator for on-chip optical interconnects, Nat. Photonics **4**, 37 (2010).

[55] G. Masada, K. Miyata, A. Politi, T. Hashimoto, J. L. O'Brien, and A. Furusawa, Continuous-variable entanglement on a chip, Nat. Photonics **9**, 316 (2015).